

Combined microslit electrokinetic measurements and reflectometric interference spectroscopy to study protein adsorption processes

Ralf Zimmermann^{a)} and Toshihisa Osaki

Max Bergmann Center of Biomaterials Dresden, Leibniz Institute of Polymer Research Dresden,
Hohe Strasse 6, 01069 Dresden, Germany

Günter Gauglitz

Institute of Physical and Theoretical Chemistry, Eberhard Karls Universität Tübingen,
Auf der Morgenstelle 8, 72076 Tübingen, Germany

Carsten Werner

Max Bergmann Center of Biomaterials Dresden, Leibniz Institute of Polymer Research Dresden,
Hohe Strasse 6, 01069 Dresden, Germany and Institute of Biomaterials and Biomedical Engineering,
University of Toronto, 5 King's College Road, M5S 3G8 Toronto, Canada

(Received 1 October 2007; accepted 29 October 2007; published 21 November 2007)

Streaming potential/current measurements for the characterization of charge formation processes at solid/liquid interfaces were combined with reflectometric interference spectroscopy. The simultaneous determination of electrostatic characteristics and the optical thickness of interfacial layers provides information on structural variations of adsorbed or covalently bound polymers and on charge dependent adsorption and desorption phenomena at solid/liquid interfaces. To demonstrate the potentialities of this extended approach for biointerfacial studies the authors report a series of experiments on the adsorption of the plasma protein fibrinogen at poly(octadecene-*alt*-maleic acid) thin films.

© 2007 American Vacuum Society. [DOI: 10.1116/1.2814066]

I. INTRODUCTION

Contact of solid surfaces with aqueous solutions very often involves the formation of interfacial charge.¹⁻⁴ In turn, electrostatic interactions were found to be relevant for a number of interfacial processes such as wetting, adsorption, and adhesion,^{5,6} the stability of proteins and nucleic acids in the vicinity of or at the interface,⁷ the kinetics of interactions between these components and biosensor surfaces^{7,8} as well as for the separation characteristics of membranes.^{9,10} Beyond that, structural characteristics of interfacial layers can be strongly influenced by the charge formation within these layers and consequently switched by the properties (*pH*, ionic strength) of the solution.^{11,12} Thus, there is a need for the comprehensive characterization of interfacial charge and structural features of interfaces.

Streaming potential and streaming current measurements are known to be useful for the investigation of charge formation processes at solid/liquid interfaces.¹³⁻¹⁵ The electrokinetic or zeta potential (ζ) derived from such measurements is defined as the electrical potential at the hydrodynamic shear plane between the solid and the bulk liquid and is often discussed in terms of models of the electrical double layer (i.e., with respect to the charge of the diffuse layer of ions compensating the surface charge). The zeta potential as a function of electrolyte solution concentration and *pH* reflects the charge formation process and can be related to the intrinsic characteristics of the solid surface. The surface conductivity (K^σ) is defined as the conductivity at the interface

caused by ion accumulation within the electrical double layer and, thus, provides complementary information on the presence and mobility of charge carriers near the surface.¹⁴

In comparison to other analytical methods, e.g., x-ray photoelectron spectroscopy, electrokinetic measurements provide direct access to the charge formation at solid surfaces in aqueous solutions. Because of this advantage, streaming potential and streaming current measurements were utilized for the *in situ* investigation of protein adsorption processes.¹⁶⁻¹⁸ Norde and Rouwendal have performed streaming potential measurements to study the adsorption of lysozyme at glass surfaces.¹⁶ In this study it was found the final zeta potential (the zeta potential at the end of the adsorption process) is rather independent of the protein solution concentration at high concentrations. This was attributed to an adsorption saturation at the glass surface. Shirahma *et al.*¹⁸ have combined streaming potential measurements and reflectometry to obtain complementary information about the kinetics of the protein adsorption and to determine the surface concentration of the protein, however the experiments were performed with uncoupled setups. Differences found by both methods were attributed to different hydrodynamic (transport) conditions in the cells used for the adsorption experiments.

To use the advantages of electrokinetic measurements for the charge formation at solid surfaces in aqueous solution and to study the influence of surface charge on interfacial processes we have developed the microslit electrokinetic setup (MES).^{19,20} The MES permits for the first time the combined determination of zeta potential and surface conductivity of flat solid surfaces. The key feature of the device

^{a)}Electronic mail: zimmermn@ipdfdd.de

substrate and the polymer (I_1) and partly at the interface between the polymer and the adjacent solution (I_2). Both partial beams show interference depending on the angle of incidence and the optical thickness of the polymer layer. A detailed comparison with other methods is given in Ref. 37.

The adsorption/desorption of biological species or a solution dependent thickness variation of the polymer layer will change the conditions for the occurrence of minima and maxima in the interference pattern. Consequently, RfS provides information of the characteristic of these processes. For more detailed information and the theoretical background of the method we refer the reader to Refs. 25 and 38.

III. MATERIALS AND METHODS

A. Sample carriers

Glass carriers ($20 \times 10 \times 3$ mm³) with layers of 40 nm tantalum oxide and 450 nm SiO₂ were purchased from Berliner Glas KGaA Herbert Kubatz GmbH & Co., Berlin, Germany. The carriers were cleaned with a mixture of aqueous ammonia solution (Acros Organics, Geel, Belgium) and hydrogen peroxide (Merck, Darmstadt, Germany) and amino-functionalized by reaction with 3-aminopropyl-dimethylethoxy-silane (ABCR, Karlsruhe, Germany).

B. Poly(octadecene-*alt*-maleic acid) films

Thin films of poly(octadecene-*alt*-maleic acid) (POMA, 50 000 g/mol) were prepared on top of the amino-functionalized sample carriers according to the following protocol:^{39,40} POMA was dissolved in tetrahydrofuran (0.08 wt %), spin-coated on the glass substrates, and annealed at 120 °C for 2 h. The anhydride moieties of the copolymer were subsequently hydrolyzed by autoclaving. The POMA was obtained from Polysciences Inc. (Warrington, PA). The thickness of the dry polymer film was determined to (4 ± 0.5) nm.

C. Electrolyte and protein solutions

All electrolyte solutions were prepared from vacuum-degassed Milli-Q water by addition of 0.1 M potassium chloride, potassium hydroxide, and hydrochloric acid solutions (Bernd Kraft GmbH, Duisburg-Neumühl, Germany). The adsorption experiments with FGN were performed in diluted phosphate buffered saline solutions (13.7 mmol/L NaCl, 0.27 mmol/L KCl, 0.81 mmol/L Na₂HPO₄, 0.15 mmol/L KH₂PO₄). The fibrinogen was purchased from Sigma (Taufkirchen, Germany).

D. Microslit electrokinetic setup

The microslit electrokinetic setup (MES) is a fully automatic instrument for the determination of zeta potential and surface conductivity of planar samples. A comprehensive description of the MES and the data evaluation is given in Refs. 19 and 20. Briefly, the instrument is characterized by the following features:

- Streaming potential and streaming current measurements are performed across a rectangular capillary system formed by two parallel sample carriers ($20 \times 10 \times 3$ mm³).
- Variability of the separation distance between two parallel sample surfaces (60 μm down to 1 μm) by means of a piezoelectric-driven positioning without dewetting of the samples.
- Laminar flow and well-defined transport conditions in the streaming channel.¹⁹
- Multi-step measurements can be performed automatically at different electrolyte concentrations and at varied slit channel height.

E. Combination of streaming potential/streaming current measurements and reflectometric interference spectroscopy

For the combination of the streaming potential/streaming current measurements (MES) with the reflectometric interference spectroscopy a VIS spectrometer (Spekol 1100, Analytik Jena AG, Germany) with a fiber optic was used.³⁰ The light of a continuous wave halogen lamp is coupled into the first arm of a bifurcated optical fiber (coupling ratio: 2:1). The end of this fiber is attached at the backside of one of the sample carriers, forming the slit streaming channel of the MES (see above). The wavelength dependent intensity pattern (resulting from the interference of the light in the thin film on top of the sample carrier) is detected with the grating detector of the VIS spectrometer. For this, the second arm of the bifurcated fiber is connected with the grating detector.

F. Calculation of the surface concentration

The optical layer thickness can be translated into the surface concentration of the adsorbed species using an approach developed by de Feijter:⁴¹

$$\Gamma = \frac{dn(1 - n_s/n)}{dn/dc}, \quad (1)$$

where d is the layer thickness, n is the refractive index of the layer, n_s is the refractive index of the solution, and dn/dc is the refractive index increment. In this study values of $n = 1.367$, $n_s = 1.333$, and $dn/dc = 0.182$ cm³/g were used for the calculation of the amount of adsorbed fibrinogen.⁴²

IV. RESULTS AND DISCUSSION

A. Charge characteristic of POMA

To study the pH-dependent charging of the POMA layer, streaming current measurements were performed in 10⁻² M KCl solutions. The dependence of the streaming current versus pressure gradient, dI_S/dp , on the pH of the electrolyte solution and the position of the isoelectric point at pH=1.9 (Fig. 3) indicate that the surface charge originates from the dissociation of the carboxylic acid groups of the polymer. Above the IEP (pH > 1.9) the magnitude of the negative streaming current increases with the degree of deprotonation of the carboxylic acid groups at increasing pH values until a

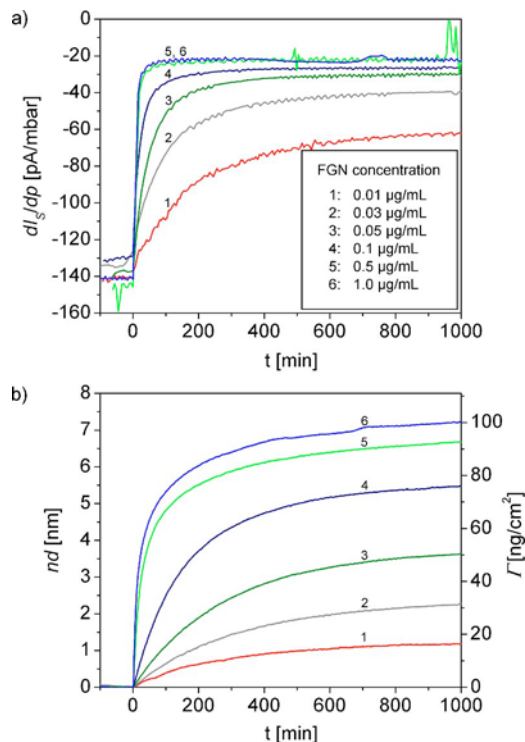


FIG. 2. Adsorption of fibrinogen at poly(octadecene-*alt*-maleic acid) films at different protein solution concentrations studied by the combination of streaming current measurements and reflectometric interference spectroscopy. Both the streaming current vs pressure gradient (a) and the optical layer thickness (b) immediately respond to the variation of the protein solution concentration. While the optical layer thickness correlates with the adsorbed amount of FGN (Γ) the streaming current vs pressure gradient reflects the variation of the interfacial charge during the adsorption process. The protein solution concentration was adjusted at $t=0$ min in the reservoir system of the MES.

plateau is reached in the basic region corresponding to the complete dissociation of the carboxylic acid groups.

B. Adsorption of fibrinogen at poly(octadecene-*alt*-maleic acid) films

The adsorption of fibrinogen onto the poly(octadecene-*alt*-maleic acid) films was studied at protein solution concentrations between 0.01 and 1.0 $\mu\text{g}/\text{mL}$ in diluted phosphate buffer solutions ($\text{pH}=7.4$). During the adsorption experiments the time-dependent variation of the streaming current versus pressure gradient and the optical layer thickness nd were recorded simultaneously (Fig. 2).

First, constant baselines of dI_S/dp and nd were confirmed for at least 1 h in the buffer solution. At $t=0$ min the desired FGN concentration was adjusted in the reservoir system of the MES. The measurements were continued up to 20 h.

The negative values of the streaming current versus pressure gradient obtained for the poly(octadecene-*alt*-maleic acid) film in the pure buffer solutions (base lines of the dI_S/dp versus t plots) can be attributed to a negative surface charge caused by dissociated carboxylic acid groups of the polymer (see above). Since the overall charge of the FGN (IEP=5.4, ..., 5.8) (Refs. 43 and 44) is negative at $\text{pH}=7.4$

as well, the FGN is adsorbed at the interface despite an electrostatic repulsion. This behavior can be attributed to hydrophobic interactions that are dominant for the protein adsorption at hydrophobic interfaces.^{45,46} However, the adsorption kinetics and the amount of protein adsorbed at hydrophobic surfaces are influenced by electrostatic interactions as well.^{47–49}

Both the streaming current versus pressure gradient and the optical layer thickness respond immediately to the variation of the protein concentration of the buffer solution at $t=0$ min. The initial adsorption rate and the slope of the dI_S/dp versus t plot increase with the protein solution concentration at low FGN concentrations. At protein concentrations higher than 0.3 $\mu\text{g}/\text{mL}$ the streaming current versus pressure gradient reaches a constant value while the related optical layer thickness (reflecting the protein surface concentration) still increases. Obviously, the electrostatic characteristics of the protein-coated surfaces level off prior to the complete saturation of the surface with adsorbed proteins. We attribute this behavior to a higher degree of preferential orientation of the adsorbed proteins to match the negatively charged polymer substrate at low protein concentrations (low adsorption rates). Due to the protein-protein interactions in the adsorbed layer interfering with the protein-substrate interaction, this electrostatically driven protein orientation is reduced with increasing protein solution concentration (surface coverage). At solution concentrations higher than 0.5 $\mu\text{g}/\text{mL}$ no further variation of dI_S/dp was observed in the plateau range of the adsorption curve. The maximum surface concentration reached at this protein solution concentration was determined to be 92.7 ng/cm^2 . This value corresponds to about 67% of the surface concentration Γ_m expected for a protein monolayer ($\Gamma_m=139.4$ ng/cm^2 if we assume a rectangular array of the adsorbed protein with lattice constants of 9 and 45 nm, respectively; dimensions of FGN: $4.5 \times 9 \times 45$ nm^3 , molecular weight: 340 000 g/mol). Since the increase of the protein solution concentration to 1 $\mu\text{g}/\text{mL}$ did not cause any further variation of the hydrodynamically accessible charge we conclude that the charged entities of the adsorbed proteins show an arbitrary orientation at $c_{\text{FGN}}=0.5$ $\mu\text{g}/\text{mL}$. Because of the modulation of the Debye screening length with the ionic strength of the solution this behavior may differ in solutions of other electrolyte compositions.

C. Charge characteristic of FGN on POMA

After reaching an almost constant optical layer thickness in the adsorption experiment the streaming channel was rinsed with 10^{-2} M KCl solutions. Subsequently the streaming current versus pressure gradient was determined for all FGN-covered POMA surfaces (Fig. 3). During the rinsing step a variation of the layer thickness of less than 5% was observed. The small variation of the layer thickness can be attributed to the decrease of the ionic strength and to a—however very limited—protein desorption.

The isoelectric point of the FGN covered POMA layers is gradually shifted toward the intrinsic isoelectric point of the

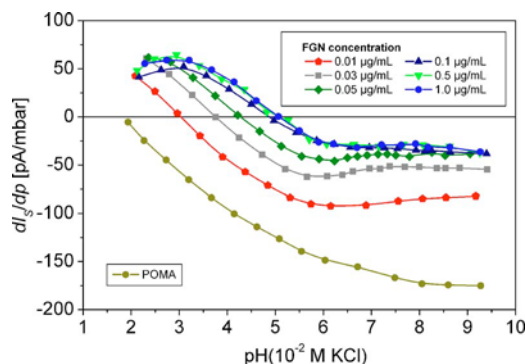


Fig. 3. Streaming current vs pressure gradient in dependence of the solution pH of a 10^{-2} M KCl solution for POMa and POMa after adsorption of FGN from solutions of different protein concentration (channel height 50 μm).

FGN (IEP=5.4, ..., 5.8) (Refs. 43 and 44) with increasing protein solution concentration up to a solution concentration of 0.5 $\mu\text{g}/\text{mL}$. At solution concentrations higher than 0.5 $\mu\text{g}/\text{mL}$ no further variation of the IEP and the dI_S/dp versus pH plot was observed, i.e., the results of the experiment are in line with the adsorption experiments (no variation of the dI_S/dp versus t plot at concentrations higher than 0.5 $\mu\text{g}/\text{mL}$). The small difference between the IEP of the FGN and the IEP of the completely covered surface can be attributed to structural variations of the protein during the adsorption process. Also, a decrease of the magnitude of the streaming current versus pressure gradient values in the alkaline pH range was observed with increasing protein solution concentrations. This effect can be related to the decrease of the net charge density at the interface with increasing FGN surface concentration.

V. CONCLUSIONS

Microslit electrokinetic measurements and reflectometric interference spectroscopy were combined to study the influence of charge formation processes on the structure and conformation of biopolymers at solid/liquid interfaces and to unravel interrelations between the interfacial charge and the formation of biopolymer layers. As compared to separate measurements, this advanced approach permits us to obtain complementary information about interfacial processes under identical and well-defined experimental conditions and to conclude on correlations between (i) charge and structure/conformation of biopolymers and (ii) charge and adsorption, desorption, and orientation of biopolymers at interfaces. To demonstrate the potentialities of the introduced methodology for *in situ* studies of the formation of biopolymer layers the adsorption of the plasma protein fibrinogen at poly(octadecen-*alt*-malic acid) films was followed at different protein solution concentrations. It was found that the orientation of the proteins at the interface is strongly influenced by the charge of dissociated groups of the maleic acid copolymer film at low protein solution concentrations. In contrast, the electrostatic characteristics approach a saturation at higher protein concentrations prior to the complete cover-

age of the surface with protein. Furthermore, the results confirm earlier findings that FGN nearly irreversibly adsorbs at hydrophobic surfaces.⁴⁷ Altogether, the results obtained point at the high relevance of surface charge for the adsorption and orientation of proteins at interfaces.

- ¹D. Myers, *Surfaces, Interfaces, and Colloids*, 2nd ed. (Wiley, New York, 1999).
- ²A. Härtl, S. Nowy, R. Zimmermann, C. Werner, D. Horinek, R. Netz, and M. Stutzmann, *J. Am. Chem. Soc.* **129**, 1287 (2007).
- ³C. Dicke and G. Hähner, *J. Am. Chem. Soc.* **124**, 12619 (2002).
- ⁴R. Zimmermann, S. S. Dukhin, and C. Werner, *J. Phys. Chem. B* **105**, 8544 (2001).
- ⁵H.-J. Jacobasch, K. Grundke, S. Schneider, and F. Simon, *J. Adhes.* **48**, 57 (1995).
- ⁶A. Bismarck, M. E. Kumru, and J. Springer, *J. Colloid Interface Sci.* **217**, 377 (1999).
- ⁷X. Liu, W. Farmerie, S. Schuster, and W. Tan, *Anal. Biochem.* **283**, 56 (2000).
- ⁸A. Baerga-Ortiz, A. R. Rezaie, and E. A. Komives, *J. Mol. Biol.* **296**, 651 (2000).
- ⁹R. van Reis, J. M. Brake, J. Charkoudian, D. B. Burns, and A. L. Zydney, *J. Membr. Sci.* **159**, 133 (1999).
- ¹⁰M. Ernst, A. Bismarck, J. Springer, and M. Jekel, *J. Membr. Sci.* **165**, 251 (2000).
- ¹¹R. Zimmermann, T. Kratzmüller, D. Erickson, D. Li, D. H.-G. Braun, and C. Werner, *Langmuir* **20**, 2369 (2004).
- ¹²R. Hidalgo-Álvarez, F. J. de las Nieves, A. J. van der Linde, and B. H. Bijsterbosch, *Colloid Polym. Sci.* **267**, 853 (1989).
- ¹³Á. V. Delgado and F. J. Arroyo, in *Interfacial Electrokinetics and Electrophoresis*, edited by Á. V. Delgado (Marcel Dekker, New York, 2001), pp. 1–54.
- ¹⁴J. Lyklema, *Fundamentals of Colloid and Interface Science* (Academic, London, 1991), Vol. II.
- ¹⁵C. Werner, R. Zimmermann, and T. Kratzmüller, *Colloids Surf., A* **192**, 205 (2001).
- ¹⁶W. Norde and E. Rouwendal, *J. Colloid Interface Sci.* **139**, 169 (1990).
- ¹⁷M. Zembala and P. Déjardin, *Colloids Surf., B* **3**, 119 (1994).
- ¹⁸H. Shirahama, J. Lyklema, and W. Norde, *J. Colloid Interface Sci.* **139**, 177 (1990).
- ¹⁹C. Werner, H. Körber, R. Zimmermann, S. S. Dukhin, and H.-J. Jacobasch, *J. Colloid Interface Sci.* **208**, 329 (1998).
- ²⁰R. Zimmermann, T. Osaki, R. Schweiss, and C. Werner, *Microfluid. Nanofluid.* **2**, 367 (2006).
- ²¹R. Schweiss, P. Welzel, W. Knoll, and C. Werner, *Chem. Commun. (Cambridge)* **2005**, p. 256.
- ²²R. Zimmermann, O. Birkert, G. Gauglitz, and C. Werner, *ChemPhysChem* **4**, 509 (2003).
- ²³R. Zimmermann, W. Norde, M. A. Cohen Stuart, and C. Werner, *Langmuir* **21**, 5108 (2005).
- ²⁴A. Härtl, S. Nowy, R. Zimmermann, C. Werner, D. Horinek, R. Netz, and M. Stutzmann, *J. Am. Chem. Soc.* **129**, 1287 (2007).
- ²⁵G. Gauglitz, J. Krause-Bonte, H. Schlemmer, and A. Matthes, *Anal. Chem.* **60**, 2609 (1988).
- ²⁶D. Beyerlein, G. Belge, K.-J. Eichhorn, G. Gauglitz, K. Grundke, and B. Voit, *Macromol. Symp.* **164**, 117 (2001).
- ²⁷G. Gauglitz, A. Brecht, G. Kraus, and W. Nahm, *Sens. Actuators B* **11**, 21 (1993).
- ²⁸J. Piehler, A. Brecht, G. Gauglitz, C. Maul, M. Zerlin, R. Thiericke, and S. Grabley, *Anal. Biochem.* **249**, 94 (1997).
- ²⁹O. Birkert, H.-M. Haake, A. Schütz, J. Mack, A. Brecht, G. Jung, and G. Gauglitz, *Anal. Biochem.* **282**, 200 (2000).
- ³⁰H.-M. Schmitt, A. Brecht, J. Piehler, and G. Gauglitz, *Biosens. Bioelectron.* **12**, 809 (1997).
- ³¹O. Birkert and G. Gauglitz, *Anal. Bioanal. Chem.* **372**, 141 (2002).
- ³²B. P. Möhrle, K. Köhler, J. Jaehrling, R. Brock, and G. Gauglitz, *Anal. Bioanal. Chem.* **384**, 407 (2005).
- ³³R. Zimmermann, C. Werner, K. J. Eichhorn, and G. Gauglitz, Patent DE 102 05 775, IPF, Universität Tübingen (7 February 2002).
- ³⁴R. Zimmermann, T. Osaki, T. Kratzmüller, G. Gauglitz, S. S. Dukhin, and C. Werner, *Anal. Chem.* **78**, 5851 (2006).

- ³⁵S. S. Dukhin, R. Zimmermann, and C. Werner, *J. Colloid Interface Sci.* **274**, 309 (2004).
- ³⁶J. F. L. Duval and H. P. van Leeuwen, *Langmuir* **20**, 10324 (2004).
- ³⁷C. Hänel and G. Gauglitz, *Anal. Bioanal. Chem.* **372**, 91 (2002).
- ³⁸G. Gauglitz, *Anal. Bioanal. Chem.* **381**, 141 (2005).
- ³⁹T. Osaki and C. Werner, *Langmuir* **19**, 5787 (2003).
- ⁴⁰T. Pompe, S. Zschoche, K. Salchert, N. Herold, M. F. Gouzy, C. Sperling, and C. Werner, *Biomacromolecules* **4**, 1072 (2003).
- ⁴¹J. A. de Feijter, J. Benjamins, and F. A. Veer, *Biopolymers* **17**, 1759 (1978).
- ⁴²J. Vörös, *Biophys. J.* **87**, 553 (2004).
- ⁴³E. G. Young, in *Comprehensive Biochemistry, Vol. 7: Proteins (Part 1)*, edited by M. Florkin and E. H. Stotz (Elsevier, Amsterdam, 1963), pp. 1–55.
- ⁴⁴P. G. Righetti and T. Caravaggio, *J. Chromatogr.* **127**, 1 (1976).
- ⁴⁵W. Norde, in *Biopolymers at Interfaces*, edited by M. Malmsten (Marcel Dekker, New York, 1998), pp. 27–54.
- ⁴⁶A. Nadarajah, C. F. Lu, and K. K. Chittur, in *Proteins at Interfaces II: Fundamentals and Applications*, edited by T. A. Horbett and J. L. Brash (American Chemical Society, Washington, DC, 1995), pp. 181–194.
- ⁴⁷C. A. Haynes and W. Norde, *Colloids Surf., B* **2**, 517 (1994).
- ⁴⁸W. Norde, *Macromol. Symp.* **103**, 5 (1996).
- ⁴⁹W. Norde and C. A. Haynes, in *Proteins at Interfaces II: Fundamentals and Applications*, edited by T. A. Horbett and J. L. Brash (American Chemical Society, Washington, DC, 1995), pp. 26–40.